Earth and Planetary Science Letters 304 (2011) 202–211

Contents lists available at ScienceDirect

Earth and Planetary Science Letters

journal homepage: www.elsevier.com/locate/epsl

Crust and lithosphere structure of the northwestern U.S. with ambient noise tomography: Terrane accretion and Cascade arc development

Haiying Gao [a,*], Eugene D. Humphreys [a], Huajian Yao [b,c], Robert D. van der Hilst [b]

[a] Department of Geological Sciences, University of Oregon, Eugene, OR, USA
[b] Department of Earth, Atmosphere, and Planetary Science, Massachusetts Institute of Technology, Cambridge, MA, USA
[c] currently at Institute of Geophysics and Planetary Physics, Scripps Institution of Oceanography, UC San Diego, La Jolla, CA, USA

ARTICLE INFO

Article history:
Received 19 August 2010
Received in revised form 30 January 2011
Accepted 31 January 2011
Available online 25 February 2011

Editor: R.W. Carlson

Keywords:
Pacific Northwest
continental growth
terrane accretion
ambient noise tomography
shear-wave velocity structure
Cascades
Siletzia

ABSTRACT

To address the tectonic and magmatic modifications of the Pacific Northwest lithosphere, including transformation of the Farallon oceanic terrane "Siletzia" into continent, we study the crust and uppermost mantle of the Pacific Northwest with fundamental-mode Rayleigh-wave ambient noise tomography using periods 6–40 s, resolving isotropic shear-wave velocity structure from the surface to 70 km depth (3 crustal layers and 2 upper mantle layers). We optimize this estimate with the aid of a neighborhood search algorithm, which we also use with receiver functions to estimate Moho depth. Horizontal node spacing is 0.25°. The EarthScope Transportable Array, the Wallowa array, a portion of the High Lava Plains array, and seven permanent stations are joined to achieve high resolution.

Very slow western Columbia Basin upper crust above very fast lower crust expresses the large Eocene sedimentary basins above a magmatically underplated crust of extended Siletzia lithosphere. High-velocity lower crust in adjacent areas to the east and south represents Siletzia thrust under the pre-accretion North America forearc. This interpretation is supported by an anomalous absence of post-accretion magmatism in these areas, implying an absence of slab removal. The southeast termination of the fast lower crust is especially strong and sharp about 35 km southeast of the Klamath-Blue Mountains gravity lineament, suggesting the Farallon slab to the southeast was torn away. The Columbia River Flood Basalts erupted at ~16 Ma, apparently creating a hole of diameter ~150 km in the edge of the underthrust Siletzia lithosphere. The magmatically active Oregon Cascade arc is slow at all depths, and the much less active Washington Cascades tend to have a volcano-centered structure that is slow in the lower crust but fast in the upper crust and upper mantle. This structure suggests that magmatic intrusion has increased upper crustal velocity, but that the higher temperatures beneath the active Oregon Cascades have a dominating effect and create low velocities.

Published by Elsevier B.V.

1. Introduction

The Pacific Northwest (PNW) of the United States coalesces a wide range of lithospheres, tectonic conditions and rock ages in a compact area (Fig. 1). In recent years the major PNW structures have become much better resolved with the deployment of EarthScope Transportable Array and several regional networks, and with the use of improved seismological methods. Existing body-wave studies image average upper mantle anisotropy (from shear-wave splitting (Fouch et al., 2008; Long et al., 2009)) and velocity structures deeper than ~100 km (teleseismic tomography of Burdick et al., 2008; Roth et al., 2008; and Schmandt and Humphreys, 2010), but do not constrain the structure of the crust and uppermost mantle. The base of the crust and lithosphere have been imaged using receiver functions (Eagar et al., 2010; Gilbert and Fouch, 2007; Levander et al., 2008), and western U.S. crust and upper mantle velocity structures have been obtained using ambient noise and tomography with EarthScope Transportable Array data (e.g., Lin et al., 2008; Moschetti et al., 2010; Yang et al., 2008).

In our PNW study of the crust and uppermost mantle we employ ambient noise tomography using about 70 more seismometers than Yang et al. (2008) to construct an isotropic 3-D shear-wave velocity model with improved resolution. We then interpret the images in a geological context to understand better the influences of Cenozoic tectonic and magmatic activity into the PNW on the structure and evolution of the lithosphere. A seismic study of this region with close consideration of its geologic history has not been done before. We focus on four major tectonic structures: (1) the boundaries and distribution of the Siletzia terrane (a large fragment of Farallon oceanic lithosphere, Fig. 1 (Duncan, 1982; Simpson and Cox, 1977; Snavely et al., 1968)); (2) the large sedimentary basins within Siletzia in south-central Washington, now largely covered by Columbia River

* Corresponding author.
E-mail address: hgao@uoregon.edu (H. Gao).

0012-821X/$ – see front matter. Published by Elsevier B.V.
doi:10.1016/j.epsl.2011.01.033

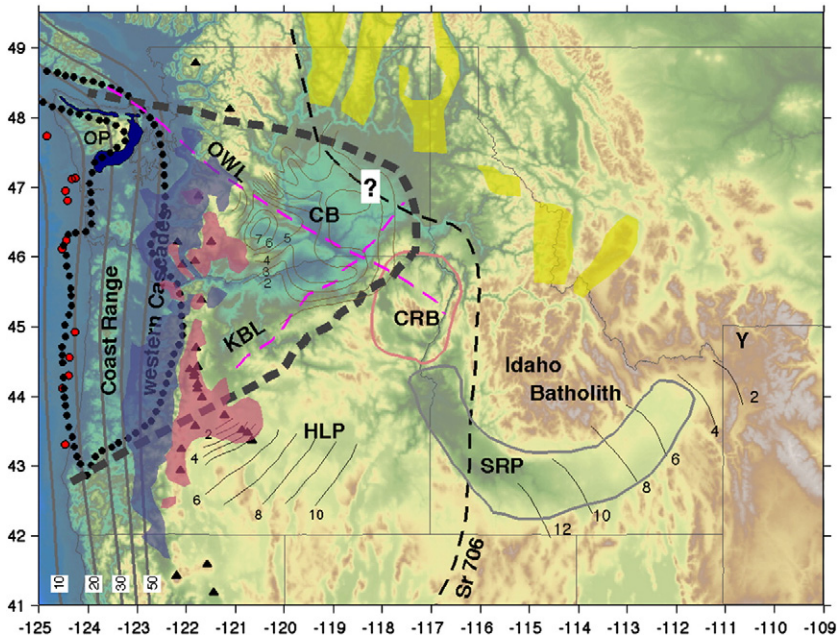

Fig. 1. Geological structures of the U.S. Pacific Northwest, including: depth contours of the Juan de Fuca plate interface at 10–50 km; outline of Siletzia west of the Cascades (black dotted line) and sampled outcrop of Siletzia (red dots) from Wells et al. (1998); our inferred outline of Siletzia (heavy gray dashes); the Olympic Peninsula (OP, Crescent Basalts in dark blue); the old western Cascades (shaded light-blue) and active High Cascades volcanic arc (shaded light-red) with Quaternary volcanoes (black triangles); the sedimentary Columbia Basin (CB) with isopach contours for Eocene basin thickness, in km (Campbell, 1989); the Klamath-Blue Mountains gravity Lineament (KBL) and Olympic-Wallowa Lineament (OWL); Cenozoic metamorphic core complexes (shaded yellow patches); isotopic $^{87}Sr/^{86}Sr$ 0.706 line (dashed black line, uncertain location in eastern Washington) that separates the accretionary terrain to the west and Precambrian North America to the east; Columbia River flood basalt source area (CRB, pink outline); Snake River Plain (SRP, gray outline); time-progressive Newberry and Yellowstone (Y) rhyolite eruptive progression across SRP and High Lava Plains (HLP) (thin black lines, in Ma); and the Cretaceous Idaho Batholith.

Flood Basalt (CRB) flows; (3) the relatively young and spatially heterogeneous Cascade volcanic arc; and (4) the source area of the CRB eruptions. We argue that Siletzia, although strongly rifted shortly after accretion (creating the large sedimentary basins), underlies much of Oregon and most of Washington including the pre-accretion forearc, that the Cascades' seismic structure reflects strong variations in advection of magma and heat, and that the CRB event occurred at the margin of accreted Siletzia and has strongly modified the seismic structure in the vicinity of Moho.

2. Geological setting

Pacific Northwest structures include the sharply truncated western margin of Precambrian North America (along the isotopic $^{87}Sr/^{86}Sr$ 0.706 line, Fig. 1 (e.g., Fleck and Criss, 1985)), onto which Mesozoic island arc and Cenozoic oceanic terranes (Simpson and Cox, 1977; Snavely et al., 1968) accreted, the Cascade volcanic arc, the ~16 Ma Columbia River Basalt flows, the extending High Lava Plains (HLP, Fig. 1) of the northern Basin and Range, the track of the Yellowstone hotspot (the Snake River Plain, SRP, Fig. 1). Most of these structures represent an episode of Cenozoic continental growth involving the intense and nearly pervasive magmatic and tectonic adjustments that followed the ~50 Ma accretion of Siletzia within the Columbia Embayment (roughly between the NE-trending Klamath-Blue Mountains gravity lineament [KBL, Fig. 1, Mann and Meyer, 1993] and the NW-trending Olympic-Wallowa structural lineament [OWL, Fig. 1, Raisz, 1945; Riddihough et al., 1986]).

Accretion of Siletzia ended a period of Laramide-age flat-slab subduction and consequent magmatic quiescence within what was previously a magmatic arc in Idaho (Idaho Batholith [Fig. 1], e.g., Gaschnig et al., 2010) and northeastern Washington (e.g., Burchfiel et al., 1992). With its accretion, subduction jumped to the western margin of Siletzia, thereby establishing the Cascadia subduction zone. Cascade arc magmatism is recognized within the Siletzia lithosphere starting about 45 Ma (Priest, 1990). Over a brief duration during or immediately following accretion, tectonic deformation switched from the compression that typified the Laramide orogeny to extension, as exemplified by metamorphic core-complex extension in northern Washington and Idaho and western Montana (Fig. 1, Foster et al., 2007). Magmatism was prolific around the accretionary boundaries of Siletzia (i.e., the Kamloops, Challis and Clarno volcanism of British Columbia and northern Washington, Idaho, and central Oregon, respectively). This new magmatic and tectonic regime represents the sudden onset of the Cordilleran ignimbrite flareup and post-Laramide extension that propagated away from this area to involve, eventually, the entire western U.S., and which is thought to be a consequence of flat-slab removal from basal North America (Coney and Harms, 1984; Coney and Reynolds, 1977; Humphreys, 1995; Schmandt and Humphreys, 2011).

The Cascade magmatic arc has been created by oblique subduction of the Juan de Fuca plate beneath North America. It is segmented in character along strike. In Oregon, the High Cascades have experienced arc-normal extension to create a discontinuous axial graben (Hughes and Taylor, 1986; Priest, 1990; Sherrod and Smith, 1990). Within this graben eruptive rates (Schmidt et al., 2008) and heat flow (Blackwell et al., 1990a,b) are high, and vents are numerous.

With intra-arc extension of the southern Cascades and Siletzia rotation about an Euler pole near the SE corner of Washington (McCaffrey et al., 2007; Wells and Simpson, 2001), the forearc has rotated clockwise at a rate of ~1°/Ma (Wells, 1990). This has transposed the older western Cascades of Oregon to its current position ~100 km west of the High Cascades. Cascade magmatic eruption rate and heat flow diminish rapidly to the north, corresponding with the decreasing intra-arc extension rate (Blackwell et al., 1990a,b). In Washington, the axis of the active High Cascades partly overlies the older western Cascades (Fig. 1) as well as uplifted pre-Tertiary basement. Along the entire length of the Cascades, heat flow is low in the older western Cascades (Blackwell et al., 1990b). The distribution of subducted sediment is irregular along the Cascade forearc Coast Ranges, but a large mass comprises the Olympic

Mountains, where sediment accumulation has uplifted the overlying basaltic crust (Crescent formation, Fig. 1), which has been lost to erosion (Brandon et al., 1998).

A third major magmatic event, following the ignimbrite flareup and the formation of the Cascade arc, began with the ~16 Ma Steens-Columbia River Basalt eruptions (e.g., Camp et al., 2003; Hooper et al., 2002). Earth's most recent flood basalt event, erupting over 200,000 km^3 of basaltic andesite and basalt that covered much of eastern Oregon and southern Washington east of the Cascades, this event is the initial Yellowstone hotspot magmatism within North America. The fissure eruptions were concentrated along a ~N–S trend in easternmost Oregon that parallels the western margin of Precambrian North America. The Columbia River Basalt eruptions occurred within a narrow swath of Mesozoic and Paleozoic terranes that lie adjacent to Precambrian North America; the basement of the Steens source area is unknown. The Columbia River Basalt eruptions are the largest and most northerly of these flood basalt eruptions, occurring at the northwestern end of what would become the Snake River Plain. Whether they have a mantle plume origin (Brandon and Goles, 1988; Camp and Ross, 2004) or are related to back-arc hydration and extension (Carlson and Hart, 1987), the magmatic activity can be expected to have modified the lower crust. Geochemical evidence places one or more large magma chambers in the lower crust (Carlson, 1984; Wolff et al., 2008), and the ~2 km of uplift focused on the Wallowa pluton during and shortly after the Columbia River Basalt eruptions indicates the loss of its dense plutonic roots at about this time (Hales et al., 2005). The Wallowa uplift lies at the center of an oscillating circular pattern of uplift and downwarp ~200-km in diameter (pink outline in Fig. 1), suggesting lithospheric modification on this scale. The circular uplift pattern and the short duration of eruptions from this area suggest significant and simply-structured changes in the crust or mantle lithosphere created by a combination of Columbia River Basalt magmatism involving lower crustal magma chambers and a (probably related) lower-crustal delamination event.

3. Data and methods

Fig. 2 shows the station distribution used in this study of the Pacific Northwest, color coded by array and comprising a total of about 280 broadband stations. These include stations from EarthScope Transportable Array, the Wallowa array, 30 stations of the High Lava Plains array, and seven permanent stations. We deployed the Wallowa flexible array of 20 broadband three-component seismometers that were borrowed from PASSCAL (Program for Array Seismic Studies of the Continental Lithosphere) in the fall of 2006 and operated the stations for two years in parts of southeastern Washington, northeastern Oregon and western Idaho. In the summer of 2008, 10 of these stations were moved to new locations to extend the array and recorded data for one additional year. The average station spacing is ~10 km for the Wallowa array along 5 short lines, ~30 km for selected High Lava Plains stations used in this study, and ~75 km for Transportable Array stations. The station coverage and deployment time overlap of these three networks from 2006 and 2009 make it possible to create a dense array and study the shallow structures in detail with ambient noise method. The seismic data are archived at and retrieved from the IRIS Data Management Center and re-sampled to 20 points/s.

In recent years the ambient noise method has been applied to measure the short and intermediate period dispersion of phase or group velocity for Rayleigh and Love surface waves (e.g., Bensen et al., 2007; Campillo and Paul, 2003; Lin et al., 2008; Moschetti et al., 2010; Shapiro and Campillo, 2004; Yang et al., 2008; Yao et al., 2006; and now, many others). Here we consider fundamental-mode Rayleigh waves recovered from ambient noise cross-correlation and estimate the phase velocity from periods 6–40 s to study the crust and uppermost mantle structures of the Pacific Northwest using the methods of Yao et al. (2006, 2008). The recovered Rayleigh-wave empirical Green functions from noise cross-correlations of continuously recorded waveforms on the vertical component between two stations are used to calculate frequency-dependent inter-station

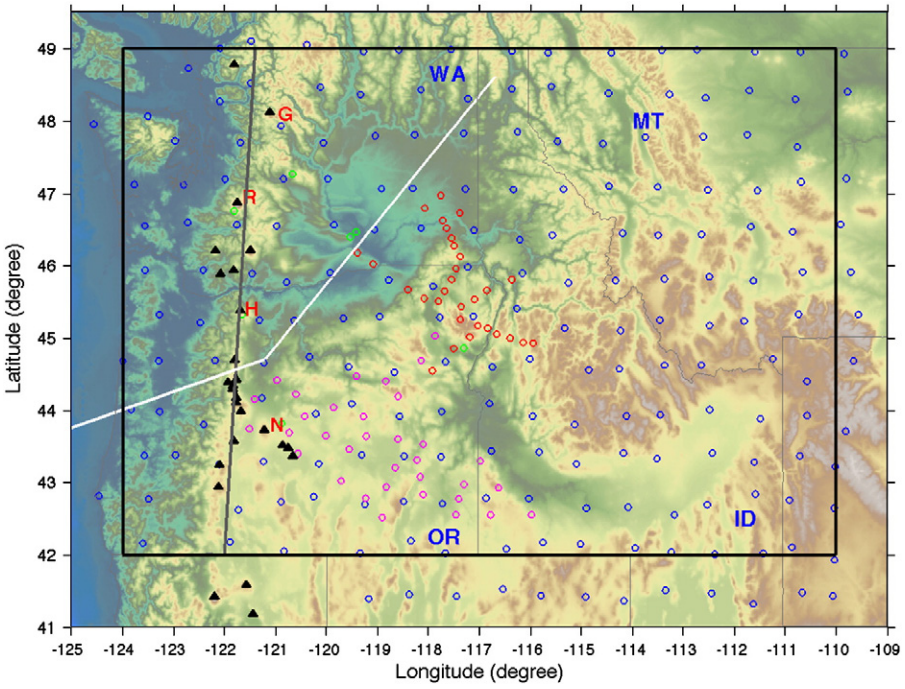

Fig. 2. The station distribution used in this study: blue circles, Earthscope USArray Transportable Array; Red circles, Wallowa flexible array; Magenta circles, 30 stations of High Lava Plains array; Green circles, 7 permanent stations. The gray line is the profile location shown in Fig. 7 and the white line is the profile of the cartoon in Fig. 8. The black rectangle is the imaging area shown in Figs. 4–6. Quaternary volcanoes (black triangles) are shown as in Fig. 1, with volcanoes as: G, Glacier Peak; R, Mt. Rainier; H, Mt. Hood; N, Newberry.

phase velocities; to satisfy the far-field approximation of surface wave propagation, we require that the inter-station distance is at least twice the wavelength. For each station pair, the cross-correlations of data from three years are stacked in order to increase the signal-to-noise ratio. The three years of data resulted in ~35,000 inter-station ray paths with a good path coverage in the study area (Fig. S1), and the farthest distance between two stations exceeds 1000 km. Using a node spacing of 0.25°×0.25°, the inter-station phase velocity dispersion curves are inverted for 2-D isotropic phase velocity maps at periods of 6–40 s. For this inversion we used the continuous regionalization method of Montagner (1986) and we choose the spatial correlation length (which controls model smoothness) as the maximum between 50 km and one-third of the wavelength for each period.

The phase velocity maps were inverted using the Neighborhood Algorithm of Sambridge (1999a,b), see Yao et al. (2008) for details, to construct a 3-D isotropic shear-wave velocity model of the crust and uppermost mantle. For our initial and reference shear-wave velocity models we use the western United States tomography model of Yang et al. (2008), which is based on ambient noise tomography and two-plane wave earthquake Rayleigh wave modeling and resolves structure to 200 km depth, and the North America upper mantle velocity model TNA of Grand and Helmberger (1984) deeper than 200 km. For Moho depth we use the initial value estimated from our receiver function study (Fig. S2), which uses the same stations that are used in our ambient noise study. Moho depth is found to vary from 22 to 55 km in the study area.

For each map node the Neighborhood Algorithm searches for the ensemble of the best-fitting 1-D models. Each 1-D model is represented by Moho depth and the velocity in five layers: the crust has three layers of thickness ratio 0.25:0.35:0.40 (from the upper to the lower crust), and there are two layers beneath the Moho, of thickness 40 km and 70 km, representing the uppermost mantle and deeper upper mantle, respectively. The shear-wave velocity is allowed to vary ±0.5 km/s in the crust and ±0.4 km/s in the uppermost mantle with respect to the reference model of each grid point. For the deepest layer, the range for shear-wave velocity perturbation is restricted to ±0.25 km/s since our dispersion data (up to 40 s) have little sensitivity to structure in that depth range. The Vp/Vs ratio is fixed at 1.76 in the crust and 1.80 in the mantle. The crustal density is calculated from empirical relationships due to Brocher (2005) and for the upper mantle layers we use a perturbation relationship given by Masters et al. (2000). Moho depth is allowed to vary by ±6 km during inversion. Using this approach, the most serious problem is the tradeoff between Moho depth and model velocities for layers near the Moho. For instance, if Moho was erroneously located too deep, lower crust and uppermost mantle velocities would be assigned velocities that were, respectively, too fast and too slow.

At each map node we first perform Neighborhood Algorithm search for these 6 parameters to identify regions of global minimum in the model space. In the second step we perform statistical analysis of the generated models to obtain the posterior mean model and the associated standard error of each model parameter (Sambridge, 1999b). Except grid points near the model margins, the Neighborhood Algorithm usually finds models that fall within given uncertainties (see example in Figs. 3 and S3). To check the reliability of the velocity model given by the Neighborhood Algorithm we perform forward calculations of dispersion from the obtained model and compare against the observed phase velocity for each grid point. The predicted phase velocities agree well with the observed phase velocities (Fig. 3).

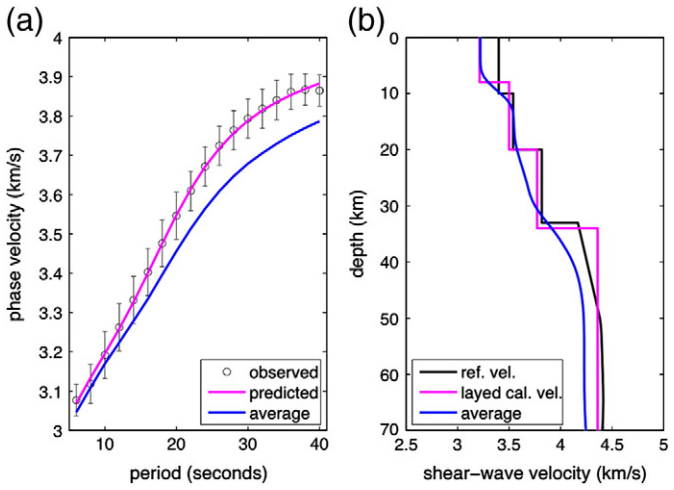

Fig. 3. Inversion result at one grid point (longitude: −117.5, latitude: 46.5). (a) Comparison of the observed (black circles with uncertainty bars) and predicted (magenta line) phase velocities estimated from the inverted shear-wave velocity (magenta line in (b)). The blue line is the average phase velocity in the studied area; (b) 1-D shear wave velocity from the surface to 70 km depth. The black line is the reference velocity model from Yang et al. (2008) at this location. The magenta line is the posterior mean layered shear-wave velocity model from the Neighborhood Algorithm (shown as vertical black lines in Fig. S3). The blue line is the average 1-D shear-wave model in the studied area.

4. Results

Our isotropic Rayleigh-wave phase velocity and shear-wave tomography results are similar to those produced with the use of only EarthScope Transportable Array data (Lin et al., 2008; Yang et al., 2008), though inclusion of the many ray paths recorded by the Wallowa and High Lava Plains flexible arrays (Fig. S1) has resulted in higher resolution of the Cascades, Siletzia and the greater source region of the Columbia River Basalts (Figs. 4–6, and S4). Average phase velocities from periods 6–40 s are ~3.05–3.78 km/s, corresponding to shear-wave velocities of 3.25–4.30 km/s from the surface to 70 km depth (Fig. 3). The average Moho depth in the study area from our receiver function estimate, at 36 km, is ~4 km deeper than that of Yang et al. (2008), resulting in significant differences in shear-wave velocity models near the Moho. Fig. 4 shows our phase-velocity perturbation maps and Fig. 5 shows the shear-wave velocity anomaly model averaged in the upper, middle, and lower crust and uppermost mantle (the model at all depths is shown in Fig. S6). Considering the variations in Moho depth in the area studied, the shear-wave velocity structure at depth between 25 and 45 km (Figs. 6 and S6) is a combination of lower crust and uppermost mantle structures in different regions. Generally, we resolve small-scale structures (~50 km) at shallow depths and uniform large-scale structures (~100 km) at lower crustal and upper mantle depths.

In a regional sense, most of Oregon except the western Cascades and northernmost part is slow in the upper crust and upper mantle, with a more complex but generally fast lower crust. This depth-alternating velocity structure is more pronounced in Idaho. In southern Idaho, velocities are slow, fast, slow for the upper crust, mid- to lower crust, and upper mantle (respectively), whereas in northern Idaho and western Montana the respective velocities are fast, slow, fast. Eastern Washington and northernmost central Oregon east of the Cascades are seismically fast at all depths, with a prominent exception of the very slow western Columbia Basin upper crust. The average crustal velocity in the 15–30 km (and especially 25–30 km) depth range (Fig. S6) is remarkably similar to surface elevation throughout the studied area, with low velocities corresponding to high elevations.

The Cascades are highly structured from the upper crust through to the upper mantle (Figs. 7 and S9). Uppermost crustal velocities in northeastern Washington display a series of north-trending low- and high-velocity stripes (Fig. 5a). These structures could be related to the similarly oriented metamorphic core complexes that experienced

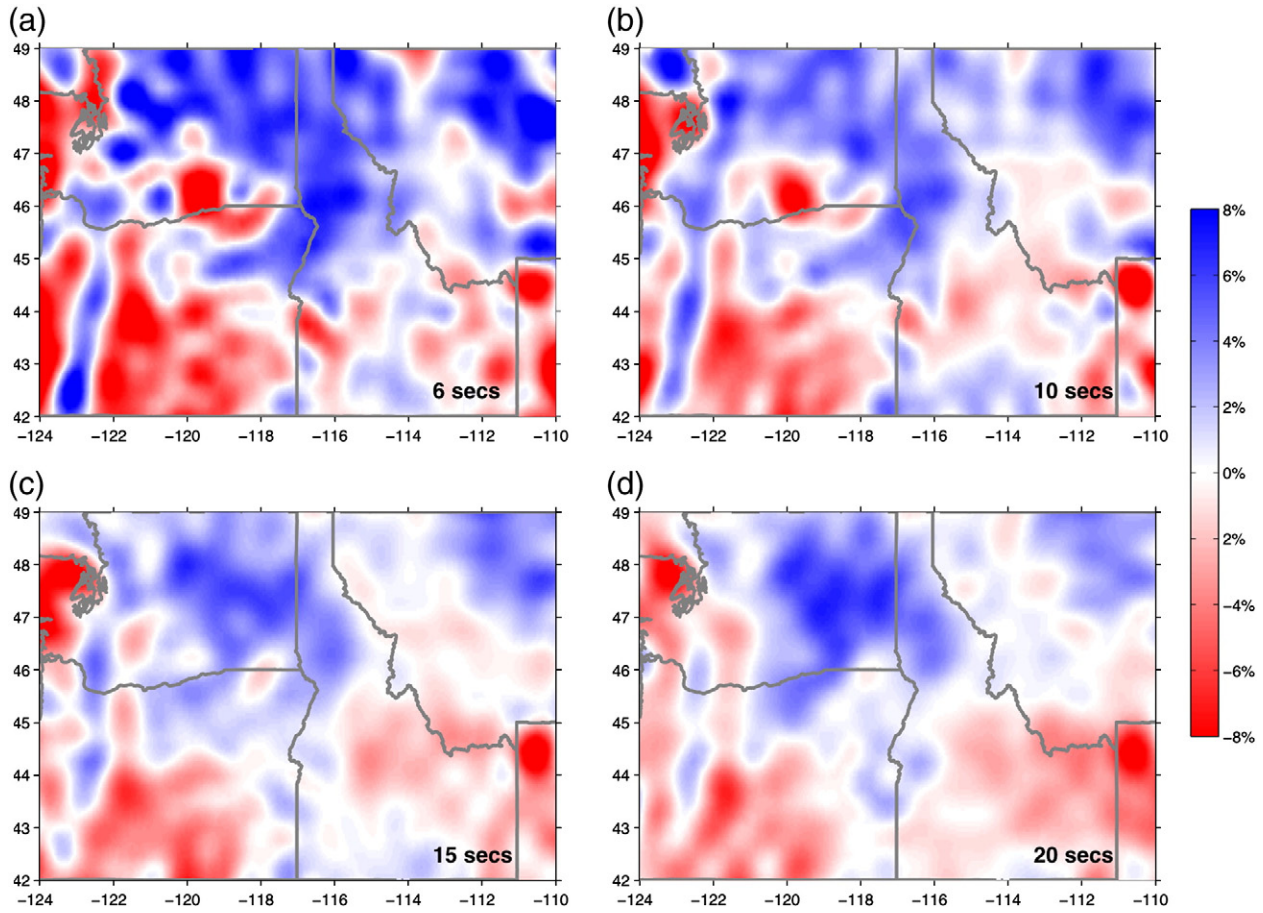

Fig. 4. Fundamental-mode Rayleigh-wave phase velocity perturbation maps at periods indicated in a range of ±8% velocity perturbation relative to the average in the studied area. Figs. 4–6 share the same color scale.

significant extension ~50 Ma across much this area and extending to near the Idaho–Montana border (yellow patches in Fig. 1, Foster et al., 2007). Below, we focus on four major structures. In chronological order of creation, these are the Siletzia terrane, the western Columbia Basin, the Cascade Mountain range, and the Columbia River Basalt source area.

4.1. Siletzia terrane

The boundaries and distribution of the oceanic Siletzia terrane are well defined west of the Cascades using geologic outcrop and a strong and distinctive magnetic pattern (outlined on Figs. 1 and 5b, Wells et al., 1998), and in this area Siletzia coincides with the area of distinctive high seismic velocity imaged in the middle crust (Fig. 5b). This is consistent with the interpretation of the Siletzia terrane as accreted oceanic lithosphere (Schmidt et al., 2008; Trehu et al., 1994). An exceptional area in and around the Olympic Peninsula is seismically slow at and above 30 km depth (Figs. S6 and S9). This low-velocity volume (as discussed by Calkins et al., 2009) is consistent with the crust being composed of off-scraped and underthrust subducted sediments (Brandon et al., 1998). The area of this low-velocity crust extends west to near the Washington coastline, roughly paralleling the subducting Juan de Fuca slab (Figs. 5, S6 and S9), but it does not extend south into Oregon, where Siletzia is imaged to increase to ~35 km in thickness (Trehu et al., 1994). At greater depths, seismic velocities are fast, consistent with the presence of the subducting Juan de Fuca slab beneath the area.

The distribution and structure of Siletzia east of the Cascades is based on indirect evidence and speculation. The strong gravity gradient across the Klamath-Blue Mountains lineament in north-central Oregon suggests an abrupt transition from the accreted Siletzia and older North America to the south. A strong and sharp seismic contrast across the Klamath-Blue Mountains lineament in north-central Oregon is in the lower crust (Figs. 5, S6 and S10), supporting the view that this lineament represents a suture between Siletzia and North America. The NE boundary of Siletzia is not exposed. The lower crust in south-central Washington and north-central Oregon is seismically very fast, whereas the upper crust is very slow and surrounded by high velocities. The area of slowest upper crust and fastest lower crust occupies the region that experienced major rifting, which is the subject of the following subsection. Adjacent to the very fast lower crust to the east and north, the lower crust and uppermost mantle is moderately fast.

4.2. Western Columbia Basin

The western Columbia Basin in south-central Washington and northernmost central Oregon is underlain by set of deep Eocene sedimentary basins (Campbell, 1989) that now are largely covered by several kilometers of Columbia River Basalt flows (Fig. S10, Reidel et al., 1989), which themselves are overlain by a thin Quaternary and Pliocene sedimentary layer. The average velocity of the upper crust beneath the western Columbia Basin is very slow (Figs. 5 and S10), consistent with preexisting views of deep sedimentary basins there (Campbell, 1989; Evans, 1994). The lower crust beneath these basins is very fast, with a velocity comparable to the upper mantle (Figs. 5 and S10). The area of very high velocity extends north farther than does the area of very low velocity upper crust, extending beneath the area of northern Washington core complexes and locally reaching the Canadian border in the lower crust and the uppermost mantle (Fig. 5).

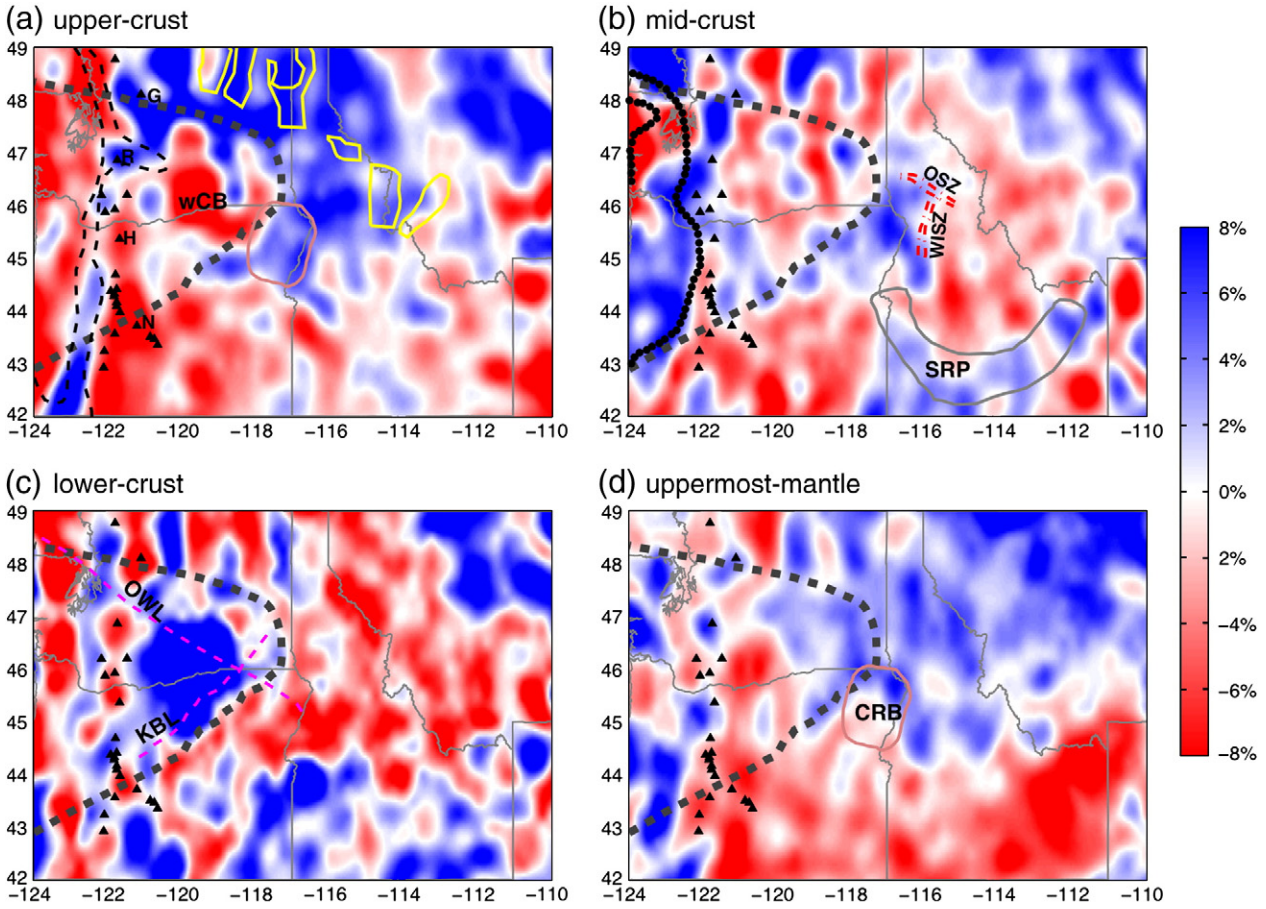

Fig. 5. Shear-wave velocity variation (in percent) with respect to the average model in the study area of the upper crust, middle crust, lower crust and uppermost mantle, respectively. Layer thicknesses vary to conform to Moho depth as shown in Fig. S2. In the crust, the thickness of each layer (from upper- to lower-crust) is laterally variable while the thickness of the uppermost mantle is set to be 40 km. The thick dashed gray line in (a–d) shows our inferred distribution of Siletzia. In (a), the black dashed line shows 40 and 50 mW/m^2 heat flow contours (Blackwell et al., 1990b). Yellow lines outline the Cenozoic metamorphic core complexes. In (a) and (d), the source area of Columbia River flood basalt is marked (CRB, pink outline). In (b), outline of western Siletzia indicated by magnetic anomalies (black dots, Wells et al., 1998) is marked, and western Idaho shear zone (WISZ, N-trending red dot-dashed lines) and Orofino shear zone (OSZ, NW-trending red dot-dashed lines) are shown. In (c), the Klamath-Blue Mountains gravity Lineament (KBL) and Olympic-Wallowa Lineament (OWL) are shown. See Fig. 1 for other structures and abbreviations.

4.3. Cascade Mountain range

The seismic structure and the magmatic and tectonic character of the Cascade volcanic arc vary strongly along strike. Seismic velocities in Oregon are slow at all depths from the upper crust to upper mantle beneath the active High Cascades volcanoes and Newberry volcano in the adjacent back-arc (Figs. 5, 7, S6 and S9). In contrast, seismic velocities beneath the Washington Cascades appear spotty with volcano-centered velocity anomaly pattern, and velocities tend to be fast, slow, fast for the upper crust, lower crust and upper mantle, respectively. Mt. Rainier (near 47°N) and Glacier Park (near 48°N) show this pattern especially well. The area south of Mt. Rainier and

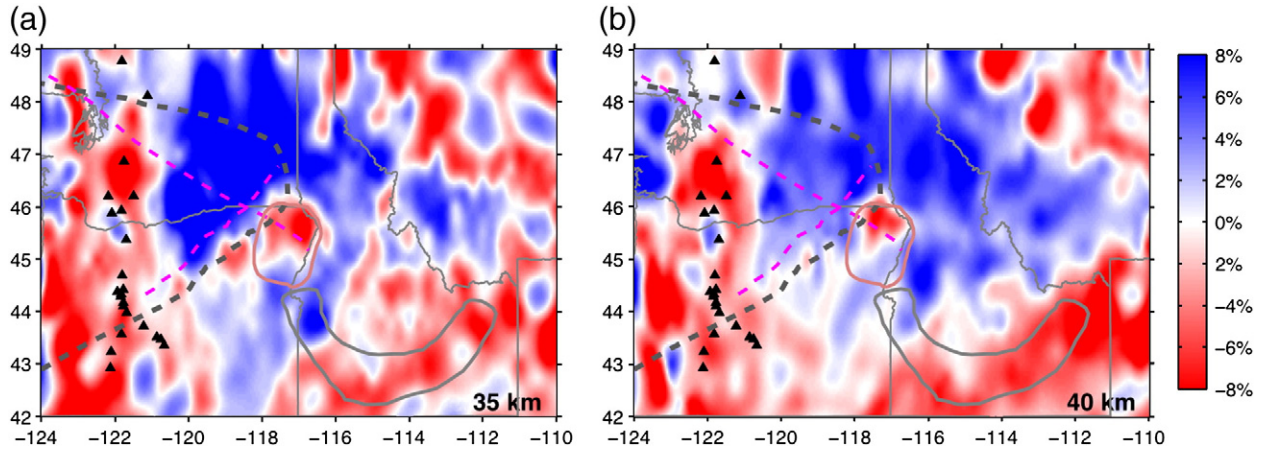

Fig. 6. Imaged shear-wave velocity anomaly model at depths 35 km and 40 km. See structures in Figs. 1 and 5.

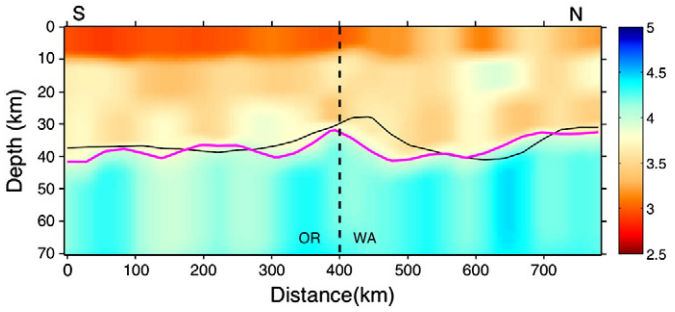

Fig. 7. Vertical cross section along the Cascade volcanic arc, showing the absolute shear-wave velocity (km/s) with depth. Fig. 2 shows profile location. Black line is the Moho interface from Yang et al. (2008), and the Magenta line is from this study. The vertical dashed line marks the state boundary between Oregon and Washington.

north of Mt. Hood is transitional in character between the northern Washington Cascades and the Oregon Cascades. The upper mantle beneath the active Cascades tends to be slow to the depth of our resolution at 50 km, with local high-velocity volumes occupying the upper mantle beneath the northern Washington Cascades.

A well-imaged trend of high seismic velocity is present in the upper and middle crust of the old western Oregon Cascades (Figs. 5 and S9). This trend extends north at 10–30 km depth with an axis near but west of the Washington Cascades. The shape of the high-velocity forearc mid-crust parallels the Cascadia subduction zone, even where the slab bends around the Olympic Peninsula (Figs. 5b and S9).

4.4. Columbia River Basalt source area

The Columbia River Basalt eruptive source area, in the NE corner of Oregon (Fig. 1), is seismically fast in the upper-to-middle crust and slow in the lower crust. Velocities are 3–5% fast at and above 20 km. The distribution of high velocities in the upper crust corresponds well with the area of Mesozoic accreted arc terranes. In the mid-crust we find a seismic contrast at the eastern margin of the Columbia River Basalt source area along west of the western Idaho shear zone, at the Precambrian margin of North America (Fig. 5b). The high velocities correlate with and may well be consequence of the Cretaceous-accreted oceanic Blue Mountains terrane, although velocities are fastest within the circular area shown in Fig. 1, especially at 20 km depth. At near-Moho depths (30–40 km, Figs. 6 and S6) beneath this circular area we image a pronounced low velocity volume (3–6% slow) that, with increasing depth, becomes slower, smaller, more northerly, and more completely surrounded by high velocity rock (Fig. S6). This is very pronounced at 35 km depth (Fig. 6), giving the appearance of a lithospheric hole beneath the main area of CRB eruptions.

5. Discussion

Continental growth is typically associated with magmatic silica enrichment processes within a volcanic arc, either within a continent or an oceanic island arc that is later accreted. Accretion of the Siletzia fragment of Farallon ocean lithosphere is related to the termination of amagmatic flat-slab subduction, initiation of the ignimbrite flareup and continental extension. The combination of these processes added area to North America and modified both North America and the accreted lithosphere itself, thereby growing and evolving a large portion of continent in ways not often considered. We use several observations relevant to the Cenozoic evolution and physical state of the Pacific Northwest to propose in the following sections that Siletzia lithosphere currently underlies much of Washington and Oregon, and suggest that the occurrence of extension around and within Siletzia was enabled by the change from compressive Laramide subduction to extension associated with rollback of the newly-established Cascadia subduction zone. Accretion of Siletzia is also thought to be responsible for the magmatic flareup that occurred around its margins as the flat-subducting Farallon lithosphere fell away (Schmandt and Humphreys, 2011) and initiated flat-slab removal that propagated away from the PNW across most of the western U.S. An illustrative cartoon (Fig. 8) is used to display the major structures discussed in the following sections.

5.1. Distribution of Siletzia lithosphere within North America

Geologic outcrop delineates well the northern and southern sutures west of the Cascades, and the NE-trending Klamath-Blue Mountains gravity lineament appears to be the southern boundary of Siletzia (Riddihough et al., 1986). The interpretation of this lineament as a suture is reinforced by the strong seismic contrast imaged across this boundary (Fig. 5) and by its along-strike extension to the mapped suture west of the Cascades (Fig. 1, Wells et al., 1998). In detail, the high-velocity lower crust and upper mantle extend 30–40 km SE of

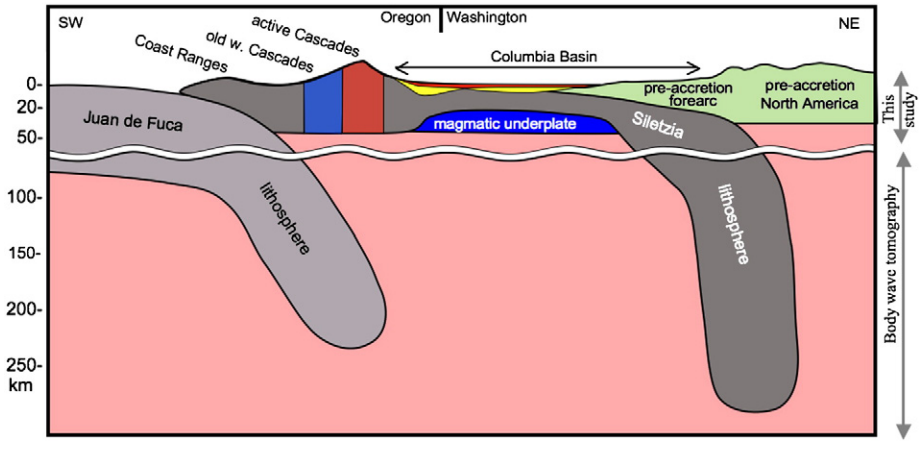

Fig. 8. Cartoon cross section illustrating the major structures inferred from our ambient-noise tomography, emphasizing the inferred distribution of Siletzia lithosphere (dark gray). Cross section location shown in Fig. 2. Structure deeper than 70 km is from body-wave tomography (Schmandt and Humphreys, 2011). Seismic velocity is fast beneath the Oregon western Cascades and slow beneath the Oregon High Cascades. The western Columbia Basin is underlain by the Columbia River flood basalts (red), deep sediment-filled Eocene basins (yellow), extended Siletzia lithosphere, and magmatic underplate (dark blue). Below the northeastern Columbia Basin, Siletzia lithosphere is shown below the pre-accretion North America crust. From the body wave tomography, Siletzia lithosphere is thought to descend vertically beneath mountainous northeastern Washington.

the Klamath-Blue Mountains lineament (Fig. 5), beneath the northern Blue Mountains, suggesting that the upper crustal and lower crustal suture are offset from one another. This suggests that Siletzia occupies a strip of lower crust and upper mantle just southeast of the inferred upper crustal suture (i.e., the Klamath-Blue Mountains lineament) and that with Siletzia accretion the flat-subducting slab to the south tore away from Siletzia. The area exposed to asthenosphere experienced the Clarno magmatism ~54 Ma (Retallack et al., 2000), ending a period of magmatic quiescence.

The major outstanding questions about Siletzia are the nature and distribution of Siletzia along its NE side. We hypothesize that Siletzia lithosphere underlies the area outlined with the gray dashed line in Fig. 1 (and Fig. 5), and that the NE margin of Siletzia underlies the pre-accretion forearc of its subduction zone. The reasons leading us to infer this extensive distribution of Siletzia lithosphere beneath much of the area east of the Cascades are: (1) Prior to Siletzia accretion Siletzia subducted beneath a forearc located between an early Cretaceous volcanic arc (trending from north-Washington Cascades to central Idaho, e.g., Gaschnig et al., 2010) and the vicinity of the Olympic-Wallowa lineament (e.g., Burchfiel et al., 1992; Christiansen and Yeats, 1992). Subduction beneath this area continued amagmatically until the time of Siletzia accretion (Geherls et al., 2009; Giorgis et al., 2005), and there is an absence of magmatic or tectonic evidence for post-accretion removal of this lithosphere. (2) The lower crust just inside of the gray dashed line in Fig. 1 (and Fig. 5c) is seismically fast compared to nearby North America lithosphere, as expected for oceanic lithosphere. The upper mantle also is fast there and farther east, beneath northern Idaho (Fig. 5d, and at 60–125 km depth from Schmandt and Humphreys, 2010), which may represent the eastward continuation of Siletzia lithosphere at greater depth. (The very fast lower crust in south-central Washington and north-central Oregon is attributed in the following sub-section to post-accretion rifting of Siletzia lithosphere.) (3) The area of fast lower crust and upper mantle spans the gap between central Washington and the seismically-inferred deeper distribution of subducted Siletzia lithosphere thought to be preserved and hanging vertically across most of the upper mantle beneath an arcuate trend extending from the north-Washington Cascades to south to central Idaho (Schmandt and Humphreys, 2011). And (4) all of eastern Washington south of the core complexes lies at low elevation (Fig. 1) and acts as a rigid block (Magill et al., 1982; McCaffrey et al., 2000) as it rotated clockwise at a rate of ~1°/Ma since accretion (Wells and Simpson, 2001; Wells et al., 1984), accompanied by Basin and Range extension within the High Lava Plains to its south, and N–S contraction along its northern side across the Yakima fold-and-thrust belt (within the forearc rocks beneath which Siletzia subducted). The nearly rigid behavior and low elevation of Siletzia, both of which are anomalous in the western U. S., are attributed to its strong oceanic rheology and high density. This behavior is expected for oceanic lithosphere that has been incorporated into a continental setting, similar to that of the Black Sea (Zonenshain and Pichon, 1986), southern Caspian Sea (Brunet et al., 2003) and western Great Valley (Godfrey et al., 1997).

5.2. Rifting origin of the western Columbia Basin

The extension that followed Siletzia accretion included both the Pacific Northwest core complexes within the mountainous areas in northern Washington and the Rocky Mountains of Idaho and Montana (yellow outlines, Fig. 1), and the area now occupied by the western Columbia Basin (wCB in Fig. 1), where extension created major sedimentary basins at low elevation (e.g., Evans, 1994) that later were covered by the Columbia River Basalt flows. Western Columbia Basin extension occurred within what we presume to be Siletzia lithosphere and overlying forearc rocks, and the timing of extension appears to be simultaneous with core-complex extension to the north, based on the contemporaneous age of bimodal volcanism.

The very slow upper crust beneath the western Columbia Basin is consistent with preexisting views of deep sedimentary basins there (Campbell, 1989; Evans, 1994). However, the sediment thickness distribution (Fig. S10a) estimated from scant outcrop and well data (Campbell, 1989) remains poorly defined, and the inferred depocenter is offset ~50 km west from a prominent Bouguer gravity high (Fig. S10b) and Columbia River Basalt thickness maximum (Fig. S10b), both of which are centered on the area of very low seismic velocity. We suspect that the actual thickness of sediment is greatest where the upper crustal velocity is lowest, and therefore exceeding the ~7 km found by drilling. Considering that mid-crustal velocities are not seismically anomalous in this region (Fig. 5b), the deepest sedimentary basins probably do not extend much below ~10–15 km depth. Away from the region of slowest upper crustal velocities, the pattern of low velocity follows well the sediment isopach map of Campbell (1989), especially on the south and east sides of the basins.

The very fast lower crust underlies the entire area of Eocene sedimentary deposition (Figs. 5c and S6 at 25–35-km depths). This structure previously was imaged beneath the Pasco Basin by Catchings and Mooney (1988), who attributed the high-velocity lower crust to mafic underplate emplaced during the Eocene extension. Our images broaden the area of inferred extension and underplating. The occurrence of Eocene metamorphic core-complex extension across elevated areas of northern Washington contrasts with the simultaneous extension of the low-lying Siletzia lithosphere, presumably reflecting compositional and density differences between the continental and oceanic lithospheres.

A switch from strong contraction during the Laramide orogeny to strong and pervasive extension occurred quickly near the time of Siletzia accretion in the Pacific Northwest (Foster et al., 2007; Van der Pluijm et al., 2006). Flat-slab subduction probably occurred prior to accretion, based on the absence of arc magmatism and the strength and inboard setting of the contraction (e.g., Feeley, 1993). With Siletzia accretion and the initiation of Cascadia subduction, the rapid onset of extension could be driven by gravitational collapse of the thickened crust (e.g., Jones et al., 1998) and enhanced by an active rollback of the newly-subducted Farallon lithosphere at Cascadia (e.g., Gurnis, 1992).

5.3. Cascades

Variations in temperature and composition relate to crustal seismic velocity in simple ways. In northern Washington, the velocity of the active Cascades upper and middle crust is fast (Fig. 5) where volcanic production rate (Schmidt et al., 2008) is low and heat flow is $\leq$40 mW/m^2 (Blackwell et al., 1990a,b). In contrast, Oregon Cascades volcanic production rate is very high, heat flow typically $\geq$80 mW/m^2 (Blackwell et al., 1990a,b) and crustal seismic velocities are very low. This set of observations suggest that magmatic intrusion of the upper crust increases seismic velocity (for Washington), but that the thermal effects of heat advection counteract this and become dominant when magmatism is strong (for Oregon). The one feature that characterizes the entire active Cascades volcanic arc is seismically slow lower crust, which could reflect the near- to super-solidus conditions there.

The older western Cascades define a zone ~100 km wide that strikes NNE across Oregon and into southern Washington, where they trend beneath the active Cascades (Fig. 1). Magmatism in the western Cascades was last active about 17 Ma, and the heat flow is low (generally $\leq$40 mW/m^2). The western Cascades middle crust shows a strong correlation between the area of high velocities and the distribution of Siletzia (Fig. 5b, Wells et al., 1998), which we attribute to the basaltic composition of Siletzia and the overlying western Cascades, along with the low temperatures.

5.4. Columbia River Basalt source area

Several major structures align with the circular pattern of uplift and downwarp (pink outline in Figs. 1 and 5) that were created during and after Columbia River Basalt eruptions (Hales et al., 2005) from this area. Considering that the magmatic volume of the CRB eruptions was very large and that the magma equilibrated at depths above ~30 km (Ramos et al., 2005), it is reasonable to infer that a large magma chamber resided within the crust beneath the topographically disturbed area and that the mantle lithosphere was lost. The seismic structure at 35–40 km (Fig. 6) images such a hole in the mantle lithosphere. Because the CRB eruptions were the first in this region since Cretaceous, we suggest that it was Siletzia lithosphere remained beneath NE Oregon until it was displaced by the CRB event.

Directly beneath the location of the topographically disturbed circular area and the anomalously low-velocity rock at 35–40 km depth, teleseismic body-wave tomography (Schmandt and Humphreys, 2011) images a hole within a patch of high-velocity mantle at 60–90 km depth, indicating that this hole extends yet deeper. At greater depth, a strongly anomalous (up to 3% P-wave velocity perturbation) high-velocity upper mantle anomaly is imaged at depths of ~125–300 km. The location of the high-velocity body beneath the apparent lithospheric hole provides a plausible accounting for the missing lithosphere. If these interpretations are correct, then the source area for the CRB event has a series of elements that are generally well aligned vertically extending from the surface to ~300 km depth, including: the main CRB dikes exposed at the surface, the mid- to lower-crustal magma chamber that fed these dikes, a patch of missing mantle lithosphere (presumably Siletzia), and the detached lithosphere. Although not understood, we note that these structures are near the Precambrian margin of North America ($^{87}Sr/^{86}Sr$ 0.706 line in Fig. 1), the presumed southern crustal suture of Siletzia (KBL in Fig. 5c) and the slab-like high-velocity body extending vertically across the upper mantle beneath Idaho (argued to be subducted Siletzia lithosphere by Schmandt and Humphreys, 2011).

6. Conclusions

Accretion of the Siletzia terrane to North America ~50 Ma abandoned a piece of oceanic lithosphere within what now is continent. Seismically imaged crust and upper mantle structure (Figs. 5, 6 and 8), when considered with the geologic record of magmatism and tectonism, supports a view that this high-velocity lithosphere remains beneath the pre-accretion forearc (the seismically-fast lower crust in Fig. 5c), was torn at its southern margin (the NE-trending sharp velocity gradient in Figs. 5c and 6a), and was strongly extended and magmatically underplated during or shortly after accretion (Fig. 8, very slow upper crust and very fast lower crust in Fig. 5). This oceanic lithosphere remains dense and strong compared to the elevated and deforming western U.S. Cordilleran in which it is embedded, although the construction of the Cascade arc and the addition of magmatic underplate and sediment fill within deep extensional basins is converting this lithosphere into continent. Thus, North America has grown through the addition and modification of oceanic lithosphere.

The accretion of Siletzia terminated flat-slab subduction beneath North America and initiated normal-dip subduction at Cascadia. This led to a sudden termination of Laramide amagmatic compression and initiation of the magmatically intense ignimbrite flareup and post-orogenic extensional collapse across the Pacific Northwest. This switch in magmatic and tectonic regime then propagated south from the site of the lithospheric tear across the western U.S., probably representing the progressive removal of the flat slab from the base of North America. Later, at ~16 Ma, the Columbia River Basalt flows appear to have created and erupted through a lithospheric hole near the torn edge of Siletzia (Fig. 6).

Supplementary materials related to this article can be found online at doi: 10.1016/j.epsl.2011.01.033.

Acknowledgements

We thank Yingjie Yang who provided the phase velocity distribution and shear-wave velocity structures of the western United States as comparison and reference. We appreciate the availability of the EarthScope's USArray Transportable Array and the permission to include a portion of the High Lava Plains project for a higher regional resolution. All data used are obtained from the IRIS Data Management Center. This project is supported by NSF awards EAR-051000 and EAR-0952194 (EH).

References

Bensen, G.D., Ritzwoller, M.H., Barmin, M.P., Levshin, A.L., Lin, F., Moschetti, M.P., Shapiro, N.M., Yang, Y., 2007. Processing seismic ambient noise data to obtain reliable broad-band surface wave dispersion measurements. Geophys. J. Int. 169, 1239–1260. doi:10.1111/j.1365-246x.2007.03374.x.

Blackwell, D.D., Steele, J.L., Frohme, M.K., Murphey, C.F., Priest, G.R., Black, G.L., 1990a. Heat flow in the Oregon Cascade Range and its correlation with regional gravity, Curie point depths, and geology. J. Geophys. Res. 95, 19,475–19,493.

Blackwell, D.D., Steele, J.L., Kelley, S., 1990b. Heat flow in the state of Washington and thermal conditions in the Cascade range. J. Geophys. Res. 95, 19,495–19,516.

Brandon, M.T., Roden-Tice, M.K., Garver, J.I., 1998. Late Cenozoic exhumation of the Cascadia accretionary wedge in the Olympic Mountains, northwest Washington State. Geol. Soc. Am. Bull. 110, 985–1009.

Brandon, A.D., Goles, G.G., 1988. A Miocene subcontinental plume in the Pacific Northwest: geochemical evidence. Earth Planet. Sci. Lett. 88, 273–283.

Brocher, T.M., 2005. Empirical relations between elastic wavespeeds and density in the Earth's crust. Bull. Seismol. Soc. Am. 95 (6), 2081–2092.

Brunet, M.-F., Korotaev, M.V., Ershov, A.V., Nikishin, A.M., 2003. The South Caspian Basin: a review of its evolution from subsidence modeling. Sed. Geol. 156, 119–148.

Burchfiel, B.C., Cowan, D.S., Davis, G.A., 1992. Tectonics overview of the Cordilleran Oregon in the western United States. In: Burchfiel, B.C., Lipman, P.W., Zoback, M.L. (Eds.), The Cordilleran Orogen: conterminous U.S.: Boulder, Colorado. Geol. Soc. Am. The Geology of North America, G-3.

Burdick, S., Li, C., Martynov, V., Cox, T., Eakins, J., Mulder, T., Astiz, L., Vernon, F.L., Pavlis, G.L., van der Hilst, R.D., 2008. Upper mantle heterogeneity beneath North America from travel time tomography with global and USArray transportable array data. Seismol. Res. Lett. 79, 384–392.

Calkins, J.A., Abers, G.A., Ekstrom, G., Creager, K.G., Rondenay, S., 2009. Imaging the slab-continent interface beneath Washington with spectral ambient noise tomography. Eos Trans. 2009AGUFM.U53A0059C.

Camp, V.E., Ross, M.E., Hanson, W.E., 2003. Genesis of flood basalts and Basin and Range volcanic rocks from Steens Mountain to the Malheur River Gorge, Oregon. Geol. Soc. Am. Bull. 115, 105–128.

Camp, V.E., Ross, M.E., 2004. Mantle dynamics and genesis of mafic magmatism in the intermontane Pacific Northwest. J. Geophys. Res. 109, B08204. doi:10.1029/2003JB002838.

Campbell, N.P., 1989. Structural and stratigraphic interpretation of rocks under the Yakima fold belt, Columbia Basin, based on recent surface mapping and well data. Geol. Soc. Am. Spec. Pap. 239, 209–222.

Campillo, M., Paul, A., 2003. Long-Range correlations in the diffuse seismic coda. Science 299, 547–549.

Carlson, R.W., 1984. Isotopic constraints on Columbia River flood basalt genesis and the nature of the subcontinental lithospheric mantle. Geochim. Cosmochim. Acta 48, 2357–2372.

Carlson, R.W., Hart, W.K., 1987. Crustal genesis on the Oregon Plateau. J. Geophys. Res. 92, 6191–6206.

Catchings, R.D., Mooney, W.D., 1988. Crustal structure of the Columbia Plateau; Evidence for continental rifting. J. Geophys. Res. 93, 459–474.

Christiansen, R.L., Yeats, R.L., 1992. Post-Laramide geology of the U.S. Cordillerian region. In: Burchfiel, B.C., Lipman, P.W., Zoback, M.L. (Eds.), The Cordilleran Orogen: conterminous U.S.: Geol. Soc. Am. The Geology of North America, vol. G-3, pp. 241–406.

Coney, P.J., Reynolds, S.J., 1977. Flattening of the Farallon slab. Nature 270, 403–406.

Coney, P.J., Harms, T.A., 1984. Cordilleran metamorphic core complexes: cenozoic extensional relics of Mesozoic compression. Geology 12, 550–554.

Duncan, R.A., 1982. A captured island chain in the Coast Range of Oregon and Washington. J. Geophys. Res. 87, 10,827–10,837.

Eagar, K.C., Fouch, M.J., James, D.E., 2010. Receiver function imaging of upper mantle complexity beneath the Pacific Northwest. US. Earth Planet. Sci. Lett. doi:10.1016/j.epsl.2010.06.015.

Evans, J.E., 1994. Depositional history of the Eocene Chumstick Formation — implications of tectonic partitioning for the history of the Leavenworth and Entiat-Eagle Creek fault system, Washington. Tectonics 13, 1425–1444. doi:10.1029/94TC01321.

Feeley, T.C., 1993. Crustal modification during subduction-zone magmatism: evidence from the southern Salar de Uyuni region (20°-22°S), central Andes. Geology 21, 1019–1022.

Fleck, R.J., Criss, R.E., 1985. Strontium and oxygen isotopic variations in Mesozoic and Tertiary plutons of central Idaho. Contrib. Mineralog. Petrol. 90, 291–308.
Foster, D.A., Doughty, P.T., Kalakay, T.J., Fanning, C.M., Coyner, S., Grice, W.C., Vogl, J., 2007. Kinematics and timing of exhumation of metamorphic core complexes along the Lewis and Clark fault zone, northern Rocky Mountains. USA. Geol. Soc. Am. Spec. Pap. 434, 207–232.
Fouch, M.J., Lin, F., Ritzwoller, M.H., West, J.D., 2008. Seismic azimuthal anisotropy beneath the western United States from ambient noise tomography and shear wave splitting. Eos Trans. 2008AGUFM.S32B..01F.
Gaschnig, R.M., Vervoort, J.D., Lewis, R.S., McClelland, W.C., 2010. Migrating magmatism in the northern US Cordillera: in situ U–Pb geochronology of the Idaho batholith. Contrib. Mineral. Petrol. 159, 863–883. doi:10.1007/s00410-009-0459-5.
Geherls, G., et al., 2009. U–Th–Pb geochronology of the Coast Mountains batholith in north-coastal British Columbia: constraints on age and tectonic evolution. Geol. Soc. Am. Bull. 121, 1341–1361.
Gilbert, H.J., Fouch, M., 2007. Complex upper mantle seismic structures across the southern Colorado Plateau/Basin and Range II: Results from receiver function analysis. Eos Trans. AGU 88 (S41B-0558).
Giorgis, S., Tikoff, B., McClelland, W., 2005. Missing Idaho arc: transpressional modification of the $^{87}Sr/^{86}Sr$ transition on the western edge of the Idaho batholith. Geology 33, 469–472.
Godfrey, N.J., Beaudoin, B.C., Klemperer, S.L., Mendocino working group, 1997. Ophiolitic basement to the Great Valley forearc basin, California, from seismic and gravity data: implications for crustal growth at the North American continental margin. Geol. Soc. Am. Bull. 109, 1536–1562. doi:10.1130/0016-7606(1997)109<1536:OBTTGV>2.3.CO.
Grand, S.P., Helmberger, D.V., 1984. Upper mantle shear structure of North America. Geophys. J. R. Soc. Lond. 76, 399–438.
Gurnis, M., 1992. Rapid continental subsidence following the initiation and evolution of subduction. Nature 255, 1556–1558.
Hales, T.C., Abt, D.L., Humphreys, E.D., Roering, J.J., 2005. A lithospheric instability origin for Columbia River flood basalts and Wallowa Mountains uplift in northeast Oregon. Nature 438 (8). doi:10.1038/nature04313.
Hooper, P.R., Binger, G.B., Lees, K.R., 2002. Constraints on the relative and absolute ages of the Steens and Columbia River basalts and their relationship to extension-related calc-alkaline volcanism in eastern Oregon. Geol. Soc. Am. Bull. 114, 43–50.
Hughes, S.S., Taylor, E.M., 1986. Geochemistry, petrogenesis, and tectonic implications of central High Cascade mafic platform lavas. Geol. Soc. Am. Bull. 97, 1024–1036.
Humphreys, E.D., 1995. Post-Laramide removal of the Farallon slab, western United States. Geology 23, 987–990.
Jones, C.H., Sonder, L.J., Unruh, J.R., 1998. Lithospheric gravitational potential energy and past orogenesis: implications for conditions of initial Basin and Range and Laramide deformation. Geology 26, 639–642.
Levander, A., Niu, F., Miller, M.S., Zhai, Y., Liu, K., Cheng, X., 2008. Receiver function images of the lithosphere in the western U.S. from USArray. Geophys. Res. Abstr. 10 EGU2008-A-12372.
Lin, F., Moschetti, M.P., Ritzwoller, M.H., 2008. Surface wave tomography of the western United States from ambient seismic noise: Rayleigh and Love wave phase velocity maps. Geophys. J. Int. doi:10.1111/j.1365-246X.2008.03720.x
Long, M.D., Gao, H., Klaus, A., Wagner, L.S., Fouch, M.J., James, D.E., Humphreys, E.D., 2009. Shear wave splitting and the pattern of mantle flow beneath eastern Oregon. Earth Planet. Sci. Lett. doi:10.1016/j.epsl.2009.09.039
Magill, J.R., Wells, R.E., Simpson, R.W., Cox, A.V., 1982. Post-12 m.y. rotation of southwest Washington. J. Geophys. Res. 87, 3761–3776.
Mann, G.M., Meyer, C.E., 1993. Late Cenozoic structure and correlations to seismicity along the Olympic-Wallowa Lineament, northwest United States. Geol. Soc. Am. Bull. 105, 853–871.
Masters, G., Laske, G., Bolton, H., Dziewonski, A., 2000. The relative behavior of shear velocity, bulk sound speed, and compressional velocity in the mantle: implication for chemical and thermal structure. Geophys. Monogr. Ser. 117, 63–87.
McCaffrey, R., Long, M.D., Goldfinger, C., Zwick, P.C., Nabelek, J.L., Johnson, C.K., Smith, C., 2000. Rotation and plate locking along the southern Cascadia subduction zone. Geophys. Res. Lett. 27, 3117–3120.
McCaffrey, R., Oamar, A.I., King, R.W., Wells, R., Khazaradze, G., Williams, C.A., Stevens, C.W., Vollick, J.J., Zwick, P.C., 2007. Fault locking, block rotation and crustal deformation in the Pacific Northwest. Geophys. J. Int. doi:10.1111/j.1365-246X.2007.03371.x.
Montagner, J.-P., 1986. Regional three-dimensional structures using long-period surface waves. Ann. Geophys. 4, 283–294.
Moschetti, M.P., Ritzwoller, M.H., Lin, F.-C., Yang, Y., 2010. Crustal shear wave velocity structure of the western United States inferred from ambient seismic noise and earthquake data. J. Geophys. Res. 115, B10306. doi:10.1029/2010JB007448.
Priest, G.R., 1990. Volcanic and tectonic evolution of the Cascade volcanic arc, central Oregon. J. Geophys. Res. 95, 19,583–19,599.
Raisz, E., 1945. The Olympic-Wallowa lineament. Am. J. Sci. 243-A, 479–485.
Ramos, F.C., Wolff, J.A., Tollstrup, D.L., 2005. Sr isotope disequilibrium in Columbia River flood basalts: evidence for rapid shallow-level open-system processes. Geology 33, 457–460.
Reidel, S.P., Tolan, T.L., Hooper, P.R., Beeson, M.H., Fecht, K.R., Bentley, R.D., Anderson, J.L., 1989. The Grande Ronde Basalt, Columbia River Basalt Group; Stratigraphic descriptions and correlations in Washington, Oregon, and Idaho. In: Reidel, S.P., Hooper, P.R. (Eds.), Volcanism and Tectonism in the Columbia River Flood-Basalt Province: Boulder, Colorado: Geol. Soc. Am. Special Paper, vol. 239.
Retallack, G.J., Bestland, E.A., Fremd, T., 2000. Eocene and Oligocene paleosols of central Oregon. Geol. Soc. Am. Spec. Pap. 344, 196.
Riddihough, R.P., Finn, C., Couch, R., 1986. Klamath-Blue Mountain lineament, Oregon. Geology 14, 528–531.
Roth, J.B., Fouch, M.J., James, D.E., Carlson, R.W., 2008. Three-dimensional seismic velocity structure of the northwestern United States. Geophys. Res. Lett. 35, L15304. doi:10.1029/2008GL034669.
Sambridge, M., 1999a. Geophysical inversion with a neighborhood algorithm—I. Searching a parameter space. Geophys. J. Int. 138, 479–494.
Sambridge, M., 1999b. Geophysical inversion with a neighborhood algorithm—II. Appraising the ensemble. Geophys. J. Int. 138, 727–746.
Schmandt, B., Humphreys, E.D., 2010. Complex subduction and small-scale convection revealed by body-wave tomography of the western United States upper mantle. Earth Planet. Sci. Lett. doi:10.1016/j.epsl.2010.06.047
Schmandt, B., Humphreys, E.D., 2011. Seismically imaged relict slab from the 55 Ma Siletzia accretion to the northwest United States. Geology 39, 175–178.
Schmidt, M.E., Grunder, A.L., Rowe, M.C., 2008. Segmentation of the Cascade Arc as indicated by Sr and Nd isotopic variation among diverse primitive basalts. Earth Planet. Sci. Lett. 266, 166–181.
Shapiro, N.M., Campillo, M., 2004. Emergence of broadband Rayleigh waves from correlations of the ambient seismic noise. Geophys. Res. Lett. 31, L07614. doi:10.1029/2004GL019491.
Sherrod, D.R., Smith, J.G., 1990. Quaternary extrusion rates of the Cascade Range, Northwestern United States and Southern British Columbia. J. Geophys. Res. 95, 19,465–19,474.
Simpson, R.W., Cox, A., 1977. Paleomagnetic evidence for tectonic rotation of the Oregon Coast Range. Geology 5, 585–589.
Snavely, P.D., MacLeod, N.S., Wagner, H.C., 1968. Tholeiitic and alkalic basalts of the Eocene Siletz River volcanics, Oregon Coast Range. Am. J. Sci. 266, 454–481.
Trehu, A.M., Asudeh, I., Brocher, T.M., Luetgert, J.H., Mooney, W.D., Nabelek, J.L., Nakamura, Y., 1994. Crustal architecture of the Cascadia forearc. Science 266, 237–243. doi:10.1126/science.266.5183.237.
Van der Pluijm, B.A., Vrolijk, P.J., Pevear, D.R., Hall, C.M., Solum, J., 2006. Fault dating in the Canadian Rocky Mountains: evidence for late Cretaceous and early Eocene orogenic pulses. Geology 34, 837–840.
Wells, R.E., Engebretson, D.C., Snavely, P.D., Coe, R.S., 1984. Cenozoic plate motions and the volcano-tectonic evolution of western Oregon and Washington. Tectonics 3, 275–294.
Wells, R.E., 1990. Paleomagnetic rotations and the Cenozoic tectonics of the Cascade Arc, Washington, Oregon, and California. J. Geophys. Res. 95 (B12), 19,409–19,417.
Wells, R.E., Weaver, C.S., Blakely, R.J., 1998. Fore-arc migration in Cascadia and its neotectonic significance. Geology 26, 759–762.
Wells, R.E., Simpson, R.W., 2001. Northward migration of the Cascadia forearc in the northwestern U.S. and implications for subduction deformation. Earth Planet Space 53, 275–283.
Wolff, J.A., Ramos, F.C., Hart, G.L., Patterson, J.D., Brandon, A.D., 2008. Columbia River flood basalts from a centralized crustal magmatic system. Nat. Geosci. 1, 177–180.
Yang, Y., Ritzwoller, M.H., Lin, F.-C., Moschetti, M.P., Shapiro, N.M., 2008. Structure of the crust and uppermost mantle beneath the western United States revealed by ambient noise and earthquake tomography. J. Geophys. Res. 113, B12310. doi:10.1029/2008JB005833.
Yao, H., van der Hilst, R.D., de Hoop, M.V., 2006. Surface-Wave array tomography in SE Tibet from ambient seismic noise and two-station analysis — I. Phase velocity maps. Geophys. J. Int. 166 (2), 732–744. doi:10.1111/j.1365-246X.2006.03028.x.
Yao, H., Beghein, C., van der Hilst, R.D., 2008. Surface wave array tomography in SE Tibet from ambient seismic noise and two-station analysis — II. Crustal and upper-mantle structure. Geophys. J. Int. 173, 205–219. doi:10.1111/j.1365-246X.2007.03696.x.
Zonenshain, L.P., Pichon, X., 1986. Deep basins of the Black Sea and Caspian Sea as remnants of Mesozoic back-arc basins. Evol. Tethys 123, 181–211. doi:10.1016/0040-1951(86)90197-6.